ORIGINAL ARTICLE

Appendicularians and marine snow *in situ* vertical distribution in Argentinean Patagonia

ELOÍSA M. GIMÉNEZ [iD] [1,†,*], ARIADNA C. NOCERA [iD] [2,3,†,*], BRENDA TEMPERONI[4,5] AND GESCHE WINKLER[6]

[1]CENTRO AUSTRAL DE INVESTIGACIONES CIENTÍFICAS (CADIC-CONICET). BERNARDO HOUSSAY 200, USHUAIA 9410, ARGENTINA, [2]CENTRO PARA EL ESTUDIO DE SISTEMAS MARINOS (CCT CENPAT-CONICET). BV. BROWN 2915, PUERTO MADRYN 9120, ARGENTINA, [3]UNIVERSIDAD NACIONAL DE LA PATAGONIA SAN JUAN BOSCO, BV. BROWN 3051, PUERTO MADRYN 9120, ARGENTINA, [4]INSTITUTO NACIONAL DE INVESTIGACIÓN Y DESARROLLO PESQUERO (INIDEP), PASEO VICTORIA OCAMPO N° 1, MAR DEL PLATA B7602HSA, ARGENTINA, [5]INSTITUTO DE INVESTIGACIONES MARINAS Y COSTERAS (IIMYC), UNMDP-CONICET, RODRÍGUEZ PEÑA 4046, MAR DEL PLATA B7602GSD, ARGENTINA AND [6]INSTITUT DES SCIENCES DE LA MER, QUÉBEC-OCÉAN, UNIVERSITÉ DU QUÉBEC À RIMOUSKI, 310 ALLÉE DES URSULINES, RIMOUSKI G5L 3A1, CANADA

*CORRESPONDING AUTHORS: eloisamgimenez@gmail.com, arinocera@gmail.com
†E.M. GIMÉNEZ AND A.C. NOCERA CONTRIBUTED EQUALLY TO THE ACCOMPLISHMENT OF THIS WORK.

Detailed *in situ* vertical and temporal distribution of appendicularians, marine snow, fecal pellets, nano- and microplankton were recorded simultaneously with environmental data in the San Jorge Gulf, Argentinean Patagonia (45°–47°S). Data were taken at a fixed station over 36 h in February 2014 with an autonomous Video Plankton Recorder and a FlowCAM®. The water column was thermally stratified with a pycnocline at ∼ 40 m. Appendicularians dominated in the upper 65 m with a condensed pattern above the pycnocline at high chlorophyll *a* concentrations, matching the subsurface chlorophyll maximum layer at ∼ 20 m. Our results suggest the absence of vertical migration of appendicularians. Marine snow, strongly correlated with appendicularians, showed high concentrations above the pycnocline, whereas fecal pellets from krill were distributed throughout the water column. Discarded houses of appendicularians or their mucus fragments were the main components of marine snow aggregates, with phytoplankton, detritus and krill pellets also contributing. Nanoplankton dominated over microplankton, with vertical distribution patterns that might depend on local grazing pressure and advective processes. Our study, the first one in the region using underwater imagery, emphasizes the leading contribution of appendicularians to marine snow aggregates in the San Jorge Gulf and their potential implications in the bentho-pelagic coupling.

KEYWORDS: *Oikopleura* spp.; marine aggregates; plankton; video plankton recorder; vertical patterns; Argentine Continental Shelf

INTRODUCTION

Appendicularians (AP) are one of the most abundant components of the mesozooplankton community (Choe and Deibel, 2008; Sato et al., 2008). They live inside a mucous structure termed a "house", secreted around the animal by its glandular epithelium, which provides protection (Alldredge, 1976). AP houses allow water filtration and retention of small colloidal food particles (Deibel, 1986; Deibel and Lee, 1992; Flood et al., 1992; Lombard et al., 2010). AP mainly prey on heterotrophic protists (flagellates and ciliates) among the nanoplankton (NP, 2–20 μm), but they can also prey on bacterioplankton and other picoplankton (PP, < 2 μm) and microplankton (MP, 20–200 μm). AP provide food to several planktonic organisms that rely on their houses and feed on the small organisms and particles trapped in the mucus (Boltovskoy, 1981). AP are attractive items for many planktonic carnivores, larvae and small adult fishes (Gorsky and Fenaux, 1998). Through predation on AP that have fed on microbial components, they link the microbial loop with the classic pelagic food web of zooplankton feeding on phytoplankton (> 20 μm; Azam et al., 1983; Fenchel, 1988; Turner, 2004). In general, AP do not exhibit a strong diel vertical migration (DVM) behavior given their low motility, thus their vertical distribution in the water column is mainly influenced by physical processes (Tomita et al., 2003; Irigoien et al., 2004; Spinelli et al., 2015).

Within the pelagic food web, and along with AP, marine snow (MS) aggregates also serve as feeding hotspots for zooplankton (Alldredge et al., 2002; Turner, 2015). These macroscopic aggregates are formed of zooplankton fecal pellets (FP), abandoned AP houses (Kiørboe, 2000), diatoms, protozoans, dinoflagellate flocs, minerals and detritus, i.e. small non-living biogenic and detrital material (Alldredge and Silver, 1988; Alldredge et al., 1993; Turner, 2002, 2015; Lundgreen et al., 2019; and references therein). Thus, MS composition is determined mainly by planktonic community structure (Lundgreen et al., 2019). Free-floating FP and MS serve as a significant additional food source for the pelagic and benthic community since consumers can profit and graze upon aggregations of small particles that otherwise are unavailable due to their size (Lampitt et al., 1993; Alldredge and Jackson, 1995). Both kinds of particles have a high nutrient content, representing a strong advantage for bacteria to colonize them (Verdugo, 2012) that, in turn, modifies the spatial and temporal dynamics of nutrients sustaining the microbial community in the water column (Wells, 1998; Belcher et al., 2016). In addition, FP and MS contribute to CO_2 sequestration, with fast-sinking rates that enhance carbon flux downward (Dunbar and Berger, 1981; Lombard and Kiørboe, 2010;

Turner, 2002; Turner, 2015). In this sense, knowledge of the composition of small particles in the water column, such as the NP and MP, is essential to better understand MS characteristics and, therefore, vertical carbon flux.

Pelagic ecosystems have a stratified vertical structure, and a wide variety of biological interactions and physical features (e.g. advective processes and tidal currents; Daly and Smith, 1993) might explain plankton and organic particle distribution (Gallager et al., 2004; McManus et al., 2005). This has considerable implications for biological productivity, water column composition, interactions and, therefore, planktonic food web dynamics (Abraham, 1998). The photic epipelagic layer is particularly interesting since it contains the ubiquitous subsurface chlorophyll maximum layer (SCML), distinctly influenced by trophic interactions (Turner, 2015). It represents a highly biologically active zone, formed and maintained by interacting processes, such as enhanced phytoplankton growth under the optimal combination of light and nutrients and photoacclimation of pigment content (Cullen, 2015). The relationship between SCML and primary consumers has been widely reported upon (Briseño-Avena et al., 2020), while it is unclear if zooplankton is found in the SCML or whether zooplankton peaks occur above it. Thorough knowledge of zooplankton DVM and thus its vertical position regarding the SCML will increase the understanding of the relationship between them. So far, studies on zooplankton distribution in the Argentine Continental Shelf (ACS) have focused mainly on the horizontal patterns (thoroughly reviewed by Cepeda et al., 2018). Less attention has been given to the in situ vertical distribution of AP and detailed information is scarce (Capitanio and Esnal, 1998; Spinelli et al., 2015).

The San Jorge Gulf (SJG, 45°–47° S, 65° 30′–67° 30′ W) is the largest semi-open basin in the ACS with a maximum depth of around 100 m. As a spawning and nursery ground for commercial fishing species, such as the Argentine hake (Merluccius hubbsi) and the Patagonian red shrimp (Pleoticus muelleri; Góngora et al., 2012), the SJG has been identified and prioritize as a strategic area by the program "Pampa Azul" of the Argentinean federal government. The Gulf contains a mixture of shelf water (salinity 33.4–33.8) and low-salinity coastal water (salinity < 33.4; Bianchi et al., 2005) that flow northwards from the Magellan Strait and Beagle Channel transported by the Patagonian Current. The SJG has been defined as an oligotrophic ecosystem that maintains high primary productivity and phytoplankton biomass turnover (Latorre et al., 2018). Remote sensing images and field studies showed elevated chlorophyll a (Chla) levels, which vary seasonally and spatially (Glembocki et al., 2015). Maximum Chla concentrations occur from austral spring until the end of
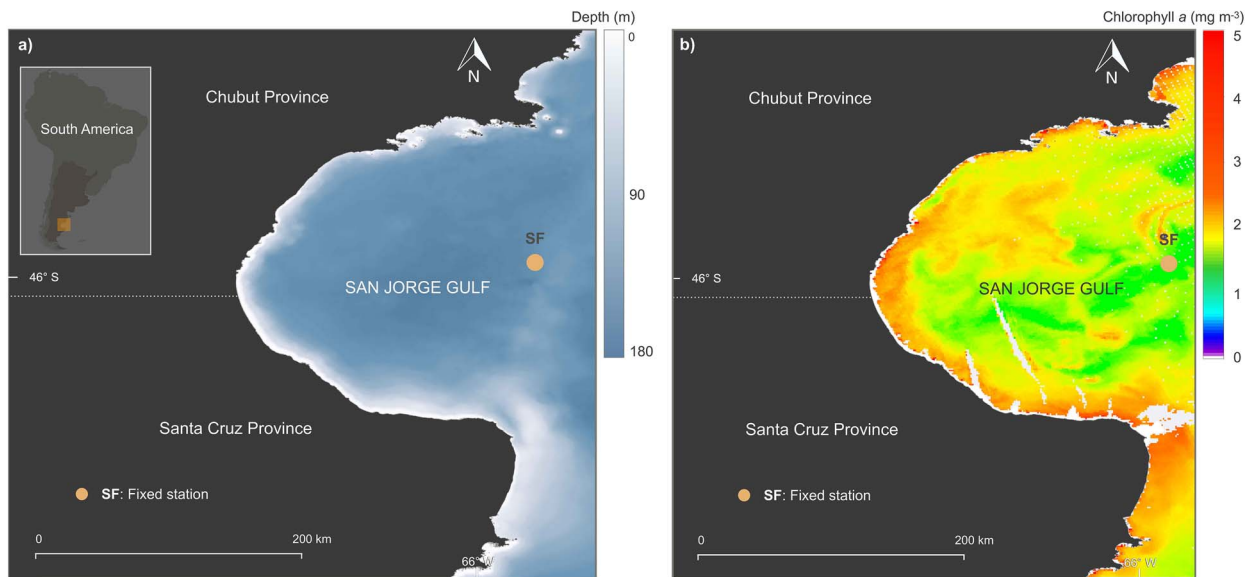
Fig. 1. Fixed station (SF) (**a**) bathymetry of the SJG (Argentinean Patagonia, South America) and (**b**) average satellite chlorophyll *a* for the area during the 36-h study period in February 2014 onboard the R/V *Coriolis II*.

summer, with a secondary maximum in autumn and a minimum in winter (Akselman, 1996; Glembocki *et al.*, 2015; Krock *et al.*, 2015). In the SJG environment, where different water masses encounter and diverse physical processes occur, a rather diverse zooplankton community develops. Their metabolism largely affects the biological carbon pump through passive sinking of exoskeletal material and FPs, or by active DVM transport from the euphotic zone to deeper water (Longhurst and Harrison, 1989; Turner, 2015).

In the SJG, AP are the second most abundant component of mesozooplankton after copepods (Pérez Seijas *et al.*, 1987; Cepeda *et al.*, 2018; Giménez *et al.*, 2018). They are a food source for the fish populations (Capitanio *et al.*, 1997, 2005). Besides, several zooplankton organisms rely on AP mucus houses, abandoned or occupied, and consume the particles retained there since, in some cases, their feeding appendage anatomy does not allow them to incorporate small particles in suspension (Esnal, 1999; Nishibe *et al.*, 2015). Despite their relevance in the food webs, no studies to date have addressed AP, FP and MS vertical distribution and only a few have studied NP and MP (Segura and Silva, 2017; Latorre *et al.*, 2018). In this context, the main goals of this study were to: (i) describe the *in situ* temporal and vertical fine-scale distribution patterns of AP, MS, FP, NP and MP in the SJG at a fixed station over a 36-h period, (ii) assess the potential ecological relationships between those components and (iii) link the observed patterns with the environmental parameters.

MATERIALS AND METHODS

Sampling procedure

This study was conducted in the framework of the multidisciplinary MARES Project (MArine ecosystem health of the SJG: Present status and RESilience capacity) on board the R/V *Coriolis II* in February 2014 in the SJG. A time-series sampling (36 h) was performed at a fixed station on February 6th, 7th and 8th (Fig. 1, Table I).

Water column characteristics

Environmental parameters such as temperature, salinity, density, Chl*a* and the attenuation coefficient (beam) were monitored using a CTD-rosette system (Sea-Bird 9 plus) with 12 L Niskin bottles. CTD was deployed 13 times throughout the sampling period, every 2 h. Fluorescence was measured using a *WetLabs ECO* sensor and calibrated by Chl*a* measurements from discrete water samples taken at four depths (surface, Chl*a* maximum, below the pycnocline and at 10 m from the seafloor) following the fluorometric technique by Parsons *et al.* (1984). All environmental parameters used to describe the water column characteristics are presented as the mean ± standard deviation.

Auto-VPR sampling and image classification

A digital autonomous Video Plankton Recorder (Auto-VPR, Seascan, Inc.), an underwater video microscope

Table I: General data of casts performed at the fixed station during the sampling period, showing the deployment location, date, and local time (UTC-3 h) for the CTD casts closest in time with the Auto-VPR deployments, local time for the Auto-VPR deployments and total seafloor depth. Bold letters denote casts performed at night

Cast number	Location		Date	CTD time (h)	VPR time (h)	Bottom depth (m)
1	45.94 S	65.62 W	6-Feb-2014	14:09	14:00	95
2	45.95 S	65.59 W	6-Feb-2014	18:13	18:30	92
3	**45.95 S**	**65.56 W**	**6-Feb-2014**	**22:14**	**22:30**	**95**
4	45.94 S	65.56 W	7-Feb-2014	12:29	12:50	90
5	45.94 S	65.57 W	7-Feb-2014	17:01	17:25	95
6	**45.95 S**	**65.56 W**	**8-Feb-2014**	**1:03**	**01:00**	**89**

system that takes images throughout the water column, was used for obtaining zooplankton images throughout the water column at the fixed station. It was deployed six times during a 36-h time frame from the surface to the bottom (∼98 m; Table I) in a continuous vertical trajectory at 40 m min^{-1}. From now on, we will refer to each deployment as "cast". Images were taken during downward and upward casts. The Auto-VPR consists of an imaging head, JPEG2000 wavelet compression processor and a hard drive for real-time recording of plankton and particles (Manual Digital Auto VPRII, 2010). It is equipped with a camera contained in a camera housing, a strobe, a main electronic housing, a recording cartridge and a battery case (Fig. 2). The camera is a 1-megapixel color camera (1024 × 1024) using a Bayer filter, Uniq model UC-1830CL. Optics were a Canon motorized zoom adapted from the J10x10R-II Lens. The frame rate of compressed images is 15 per second, and the maximum rate of the strobe is 30 flashes per second, with an energy of 1 joule per flash. Its duration is in the order of 3.0 ms. The data were obtained using the lowest magnification (S3), which images an optical field of view of 42 × 42 mm. The low magnification cameras are designed for larger and rarer taxa (Davis et al., 1992; Benfield et al., 1996). Each video frame imaging volume ranged from 0.62 to 147 cm^3. The AutoDeck software allowed us to sort the images of organisms and particles detected by the VPR camera in the water column. The software reads each data block, separates and decodes the header, decompresses the image and scans it for a region of interest (ROI). The basic processing of AutoDeck is to extract sub-images that are reasonably sharp to be able to identify the represented object. To set the focus (structure) of sub-images, the program looks at the light gradient (sobel) and high-frequency content (standard deviation control; Manual Digital Auto VPRII, 2010). The extraction parameters we used were: a sobel of 11, a standard deviation of 10%, a growth scale of 302% and segmentation thresholds low and high of 0 and 150, respectively.

Then, Auto-VPR images were selected while manually scrolling through the list of images obtained. Any plankton or particle images judged to be in focus were identified by the observer and classified as AP, FP and MS. Some of the extracted images were not in focus and therefore did not allow identification; these were not considered in the analysis. We defined the macroscopic aggregates in our images as MS, mainly originated from AP' discarded houses (Alldredge and Silver, 1988), whereas FP of our images were identified as euphausiid ones (Atkinson et al., 2012; Gleiber et al., 2012). To estimate the contribution of AP houses to the MS concentration, the relationship between house renewal rate and temperature was used (Sato et al., 2001).

FlowCAM® imaging

Discrete samples were obtained from the rosette system from three depths (surface, Chl*a* maximum and bottom) in each of the six casts. They were preserved in acid Lugol's solution (Parsons et al., 1984) and stored in amber glass bottles in the dark at 4°C for further analysis in the laboratory. The surface sample of Cast 4 was lost due to preservation problems. A total of 17 samples were analyzed to identify NP and MP. Samples were analyzed with a B/W FlowCAM®TM II benchtop instrument (Fluid Imaging Technologies, Scarborough, ME, USA), using the software package Visual SpreadSheet (VISP) version 1.5.16. All measurements were done using the automatic imaging mode. A 10× objective was used in the FlowCAM®, and the dimension of the flow cell, determined by the objective, was 2 × 0.1 mm (10×) flow cell. The automatic mode seems most useful for whole plankton community assessments and, depending on the lens used, is limited by the rather low sample volume processed (Jakobsen and Carstensen, 2011). The images were sorted by visual inspection, and particles in the 4–500 μm range were analyzed.
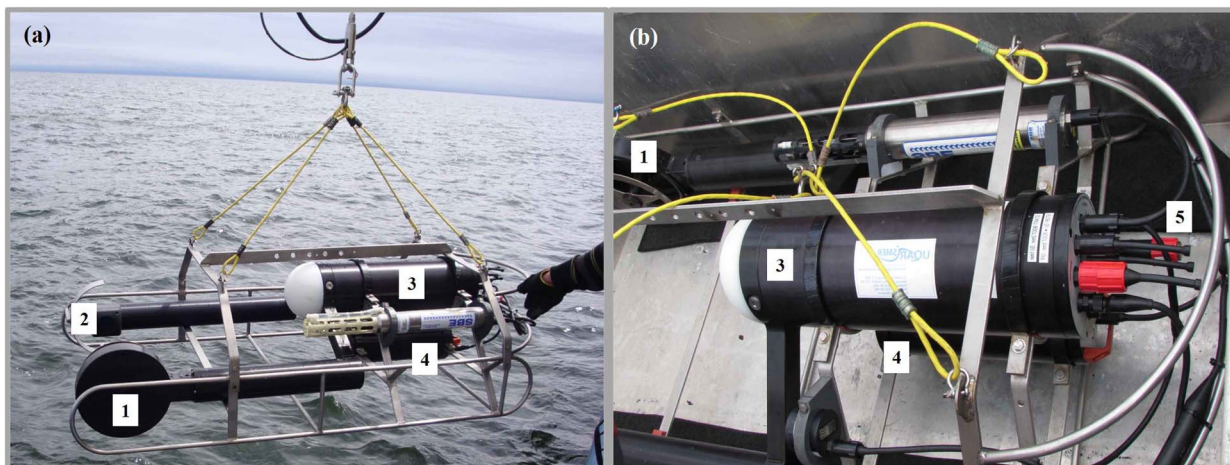
Fig. 2. (**a**) Deployment of the Auto-VPR during the sampling at a fixed station in the SJG in Argentine Patagonia in February 2014. (**b**) Details of Auto-VPR parts. (1) Strobe, (2) camera housing, (3) main electronic housing, (4) battery case, (5) recording cartridge.

Data processing and statistical analyses

All ROIs of AP, FP and MS obtained by Auto-VPR were matched with time and depths. The concentrations of the different items were calculated using the *vprr* package in R software (R Development Core Team, 2019). For all vertical casts, the presence of different items (AP, MS, FP, NP and MP) was presented as average abundances (individuals or particles m^{-3} and cells mL^{-1}) for every 1-m depth interval to evaluate their distribution in the water column. Normality and homoscedasticity were checked by the Shapiro test. If normality was not met, data were normalized with a logarithmic transformation. Then, Spearman's and Pearson's correlations were performed between all biological variables (AP, MS, FP, NP and MP) and environmental parameters and biological variables, respectively. We conducted a General Linear Mixed Model (GLMM) analysis to explain AP, MS and FP concentrations in relation to environmental parameters (fixed effects) and cast number (random effect) using *lme4* package from R Statistical Software (R Development Core Team, 2019). To test the significance of a random effect, we performed a likelihood ratio test. We used the data of CTD casts closest in time with the Auto-VPR deployment to minimize the error (Table I). We considered strong correlation if the module coefficient value ranged between 0.50 and 1; moderate correlation if the value ranged between 0.30 and 0.49; and weak correlation if the value lied below 0.29. The significant threshold for the observed differences was considered at a *P*-value < 0.05. All organisms, particles and cells concentrations, as well as the environmental parameters values are presented as the mean $\pm$ standard deviation.

RESULTS

Water column characteristics

The CTD data indicated a thermally stratified water column with an upper mixed layer above 40 m (Fig. 3). Temperature's transition was evident at 40 m depth, showing $\sim 14°$C at the surface and decreasing to 9°C at the bottom. Salinity decreased from 33.25 psu near the surface to a less saline (~ 33.12 psu) mid-layer between 40 and 60 m, increasing again with depth, reaching ~ 33.30 psu near the seafloor. Density values increased with depth, ranging between ~ 24.8 and 26.1 kg m^{-3} and showed a pycnocline at ~ 40 m, with temperature being the most important parameter to define it. A SCML occurred between 15 and 35 m, with a peak of 1.2 mg m^{-3} at ~ 25 m. The attenuation coefficient (beam) showed similar percentages for the upper 40 m; below this depth, values decreased with a marked decline below 60 m, reaching 60% near the bottom.

Auto-VPR data: appendicularians, marine snow and fecal pellets

Defined images (Fig. 4) and fine-scale distribution of AP, MS and FP were detected from the Auto-VPR data in all daytime and nighttime casts (Table I). A total of 3762 images were classified for the analyses (Table II), corresponding to AP (N = 1449), MS (N = 829) and FP (N = 1484). The Cast 6 showed the lowest total classified images and integrated concentrations of all casts for AP, MS and FP (Table II). Average concentrations were 105.83 ± 253.64 ind m^{-3}, 50.66 ± 102.06 particles m^{-3} and 112.11 ± 165 FP m^{-3}, respectively, showing

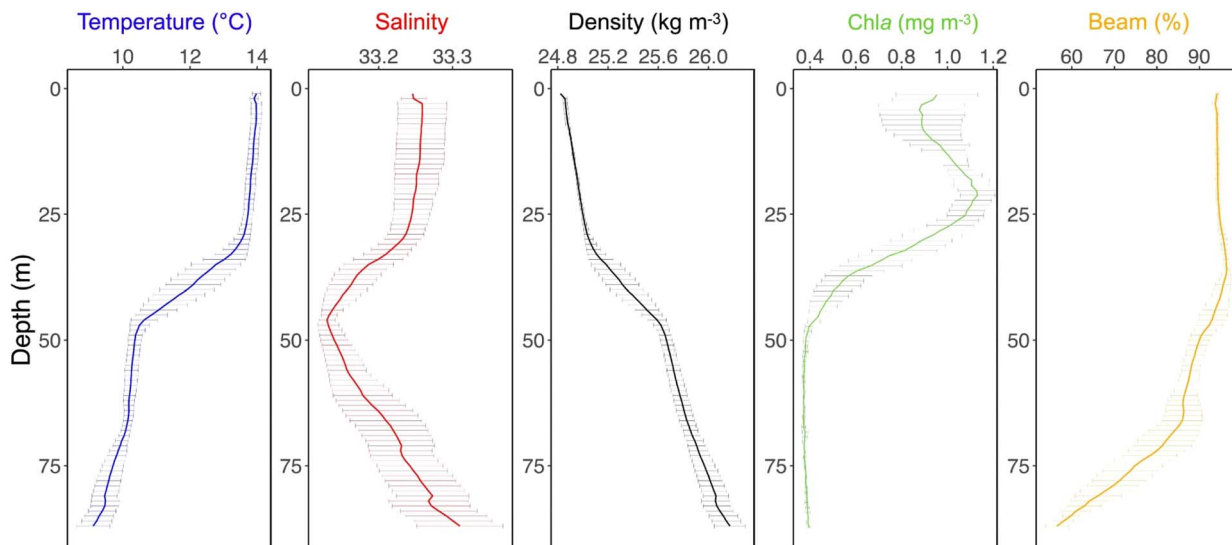**Fig. 3.** Average ± standard deviation for the 13 vertical CTD profiles (from left to right): temperature (°C, blue line), salinity (psu, red line), density (kg m^{-3}, gray line), chlorophyll *a* (Chl*a*, mg m^{-3}, green line) and the attenuation coefficient (Beam in %, orange line).
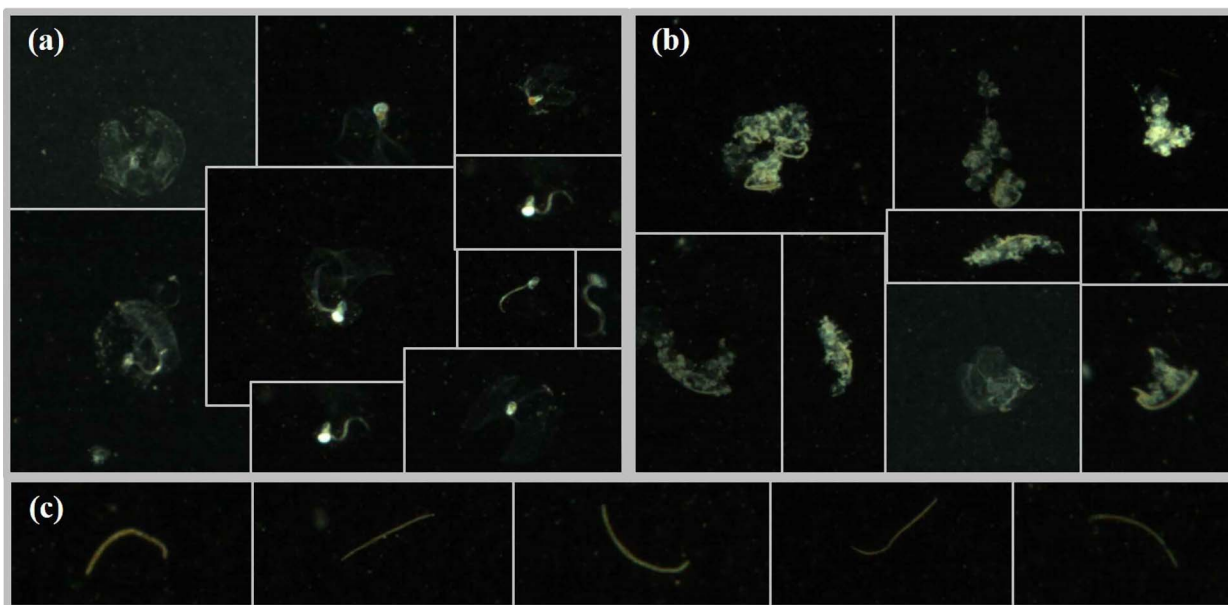

Fig. 4. Examples of (**a**) appendicularians, (**b**) marine snow and (**c**) fecal pellets images from the Auto-VPR in the SJG. Note that in most cases, the ROIs are not on the same scale.

temporal variability in their overall abundances and vertical distributions among casts.

The average concentration of AP (Fig. 5a) ranged from 0.44 ± 4.03 (Cast 6) to 301.54 ± 395.86 ind m^{-3} (Cast 3), with a maximum registered value of 1975.13 ind m^{-3} (Cast 1). In casts with a high concentration of AP (Casts 1, 3, 4), peak concentrations coincided with the SCML positioned above the pycnocline. This pattern was less pronounced when mean concentrations were low (Casts 2, 5, 6). AP were widely spread between 2 and 65 m. In general, no specific distribution pattern could be associated to day or night.

MS average concentrations (Fig. 5b) varied between 10.18 ± 21.6 (Cast 6) and 167.7 ± 179.7 particles m^{-3} (Cast 3), with a maximum concentration of 748.6 particles m^{-3} (Cast 3). Vertical distribution showed at high

Table II: List of classified items showing the number of images analyzed (NI, low magnification camera), integrated concentrations (IA, ind/particles/FP m⁻²) and total image volume (V, m⁻³) for all the Auto-VPR casts. AP = appendicularians, MS = marine snow, FP = fecal pellets

Item	Cast number												Total
	1		2		3		4		5		6		
	NI	IA/V	NI	IA/V	NI	IA/V	NI	IA/V	NI	IA/V	NI	IA/V	
AP	257	249.6/1.93	47	10.8/1.95	905	305.4/1.71/	238	86.8/1.48	1	1.35/7.96	1	0.45/1.77	1 449
MS	100	44.4/1.81	68	21.8/2.0	478	170.2/1.74	105	44.5/1.48	47	26.6/0.76	31	10.3/1.77	829
FP	447	294.3/1.98	117	31.5/2.0	455	146.8/1.74	431	160.9/1.49	31	46.1/8.54	3	0.86/1.77	1 484
Total items	804		232		1838		774		79		35		3 762

concentrations an agglomeration above the pycnocline (Casts 3 and 5). In contrast, at medium concentrations, MS was distributed homogenously throughout the water column (Casts 1 and 4).

The house renewal rate for integrated AP concentrations gave as result the same order of magnitude for half of the casts when compared with MS integrated concentrations (Casts 1, 4 and 6). The Cast 1 showed the highest relationship with house production (124.5%) representing more than the MS integrated concentration found (55.3 houses m⁻² vs. 44.4 particles m⁻²). In contrast, AP house production only represented 0.9% of MS concentration found in Cast 6 (0.1 houses m⁻² and 0.86 particles m⁻²). For the remaining casts, MS concentration was one order of magnitude higher than the one for AP (21.8 houses m⁻² vs. 2.5 particles m⁻² and 170.2 houses m⁻² vs. 67.7 particles m⁻², for Casts 2 and 3, respectively), whereas for Cast 5 the MS integrated concentration was two orders higher than AP produced houses (26.6 houses m⁻² vs. 0.3 particles m⁻²).

FP vertical distribution did not show peak concentrations either with the SCML or the pycnocline throughout the 36-h survey (Fig. 5c). FP concentrations were generally distributed throughout the entire water column, except for Casts 5 and 6. Average concentrations ranged between 0.85 ± 4.45 (Cast 6) and 291 ± 237.78 FP m⁻³ (Cast 1), and the highest concentration was 1219.9 FP m⁻³ (Cast 1).

Furthermore, in Auto-VPR images, a dense layer of small particles (Supplementary Fig. S1), identified by us as detritus, was observed below the pycnocline until the bottom in Casts 1 (52–83 m), 3 (49–78 m) and 4 (47–85 m).

FlowCAM® imaging: nano- and microplankton

NP and MP were composed of ciliates, flagellates (mostly found in the surface sample) and other phytoplankton (G. Ferreyra, Ushuaia, personal communication)

(FlowCAM® images, Supplementary Fig. S2). The dominant group size was the NP. Vertical distribution showed a maximum concentration of NP and MP at the bottom in every cast except in Cast 6 maximum MP concentrations were found at the surface (Fig. 6). During the sampling period, NP concentrations varied from 839 cells mL⁻¹ at the surface in Cast 2 to 14 835 cells mL⁻¹ at the bottom in Cast 1. MP ranged from 6 cells mL⁻¹ at the surface in Cast 3 to 630 cells mL⁻¹ at the bottom in Cast 6, the former being two orders of magnitude higher than the latter. When all casts and depths were considered, NP presented higher concentrations than MP (4463.71 ± 5145.24 cells mL⁻¹ and 173.59 ± 187.17 cells mL⁻¹, respectively), the former with great variability and showing the highest concentrations near the bottom (11677.67 ± 815.37 cells mL⁻¹; Fig. 6). Surface cells were in a good physiological state (Supplementary Fig. S2a), and bottom depth images revealed degraded cells and organism fragments (Supplementary Fig. S2b; G. Ferreyra, Ushuaia, personal communication).

Relationships of plankton, marine snow and fecal pellets with the environmental parameters

Some strong and moderate correlation coefficients were recorded between AP, MS and FP, and environmental parameters (Table III). All biological variables (i.e. AP, MS, FP, NP and MP) were strongly correlated with temperature, showing the highest positive value with AP ($r^2 = 0.59$) and the highest negative value with MP ($r^2 = -0.67$). Likewise, for the beam attenuation coefficient, all biological variables were highly correlated, except the MP. The strongest negative correlation coefficient was found for NP ($r^2 = -0.77$), followed by a positive and strong correlation with MS ($r^2 = 0.75$). Regarding density, three biological variables were strongly correlated, from higher to lower relationships: NP ($r^2 = 0.67$), MP ($r^2 = 0.66$) and MS ($r^2 = -0.5$).
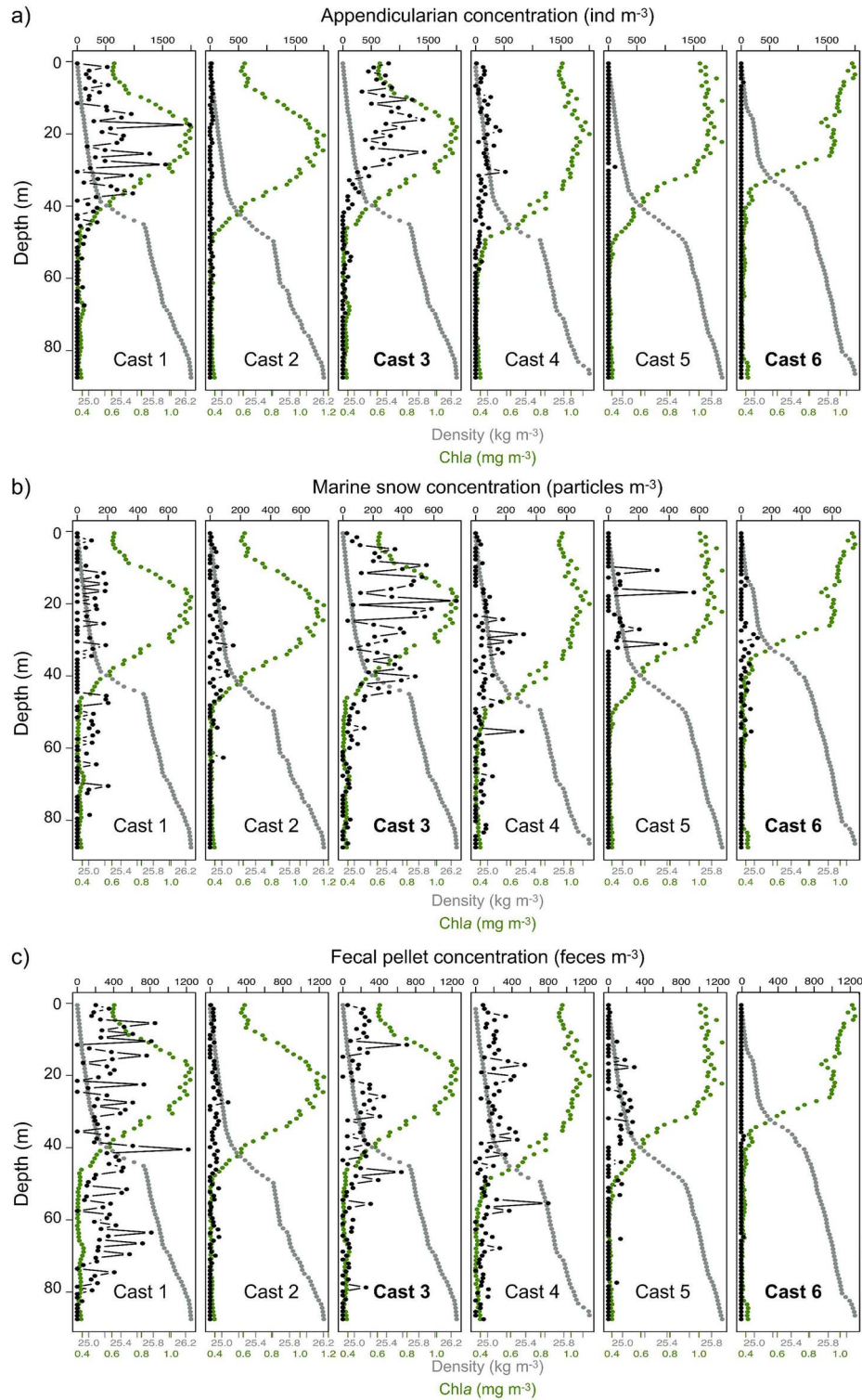
7

Fig. 5. Vertical distribution obtained from the Auto-VPR sampling for (**a**) appendicularians (ind m^{-3}, black dots), (**b**) marine snow (particles m^{-3}, black dots) and (**c**) fecal pellets (FP m^{-3}, black dots) during the 36-h survey at the fixed station in the SJG in February 2014. In addition, profiles from CTD for chlorophyll *a* (Chl*a*, mg m^{-3}; green dots) and density (kg m^{-3}; gray dots) are shown on each panel for the same period and deployed casts (6 times). Nighttime casts (3 and 6) are indicated in bold.
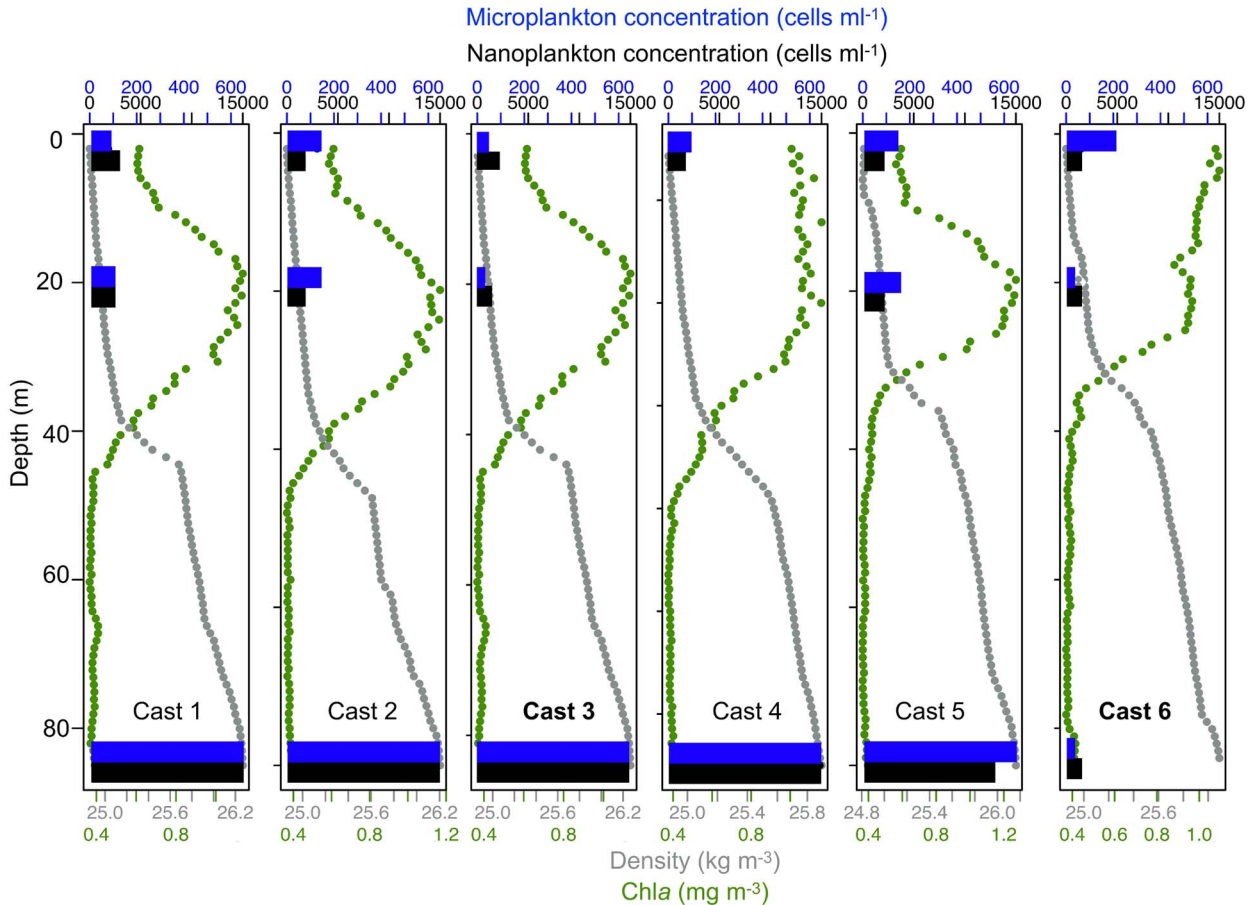
Fig. 6. Total concentrations of nano- (cells mL^{-1}, black bars) and microplankton (cells mL^{-1}, blue bars) provided by the FlowCAM$^{®}$, chlorophyll *a* (Chl*a*, mg m^{-3}; green dots) and density (kg m^{-3}; gray dots) vertical profiles for each cast obtained from the Niskin bottles. Three samples were taken at different depths for the FlowCAM$^{®}$: surface (2 m), subsurface chlorophyll maximum (20 m) and bottom ($\sim$83 m).

Table III: Spearman's correlation coefficients among the biological variables: appendicularians (AP), marine snow (MS), fecal pellets (FP), nanoplankton (NP) and microplankton (MP) and environmental parameters considering three discrete depths (surface, chlorophyll a maximum and bottom) and the six casts

	Temperature	Salinity	Density	Chl*a*	Beam
AP	0.59	−0.001	−0.49	0.37	0.54
MS	0.54	−0.18	−0.50	0.46	0.75*
FP	0.54	0.12	−0.44	0.26	0.57
NP	−0.53	0.44	0.67	−0.59	−0.77*
MP	−0.67	0.29	0.66	−0.40	−0.43

Underlined numbers indicate strong correlations (r^2 > 0.5). Significant correlations (*P* < 0.05) are indicated with asterisks (*). Chla = chlorophyll a; Beam = attenuation coefficient.

Chlorophyll *a* only presented a strong correlation coefficient with NP. The remaining correlation relationships were weak/moderate (lower than 0.50).

Analyzing just biological variables, Spearman's correlation coefficients showed strong and positive correlations among AP, FP and MS (Table IV). NP and MP also presented a high correlation coefficient, followed by strong negative correlations with MS in both cases.

Chl*a* was the most important factor determining the spatiotemporal dynamics of AP, MS and FP (Table V). Results of the GLMM when AP, MS and FP were considered as a continuous record data showed that Chl*a* concentrations best explained the vertical distribution of AP, MS and FP. In addition, the models also showed that MS and FP concentration was related with beam. FP concentrations were also associated with temperature

9

Table IV: Spearman's correlation coefficients for AP, FP, MS, NP and MP for the surface (2 m), chlorophyll a maximum (20 m) and bottom (83 m) discrete samples and all casts (from 1 to 6). AP = appendicularians, MS = marine snow, FP = fecal pellets, NP = nanoplankton, MP = microplankton

	AP	MS	FP	NP	MP
AP	1	0.91*	0.92*	−0.40	−0.48
MS		1	0.86*	−0.45	−0.47
FP			1	−0.52	−0.50
NP				1	0.61*
MP					1

Underlined numbers indicate strong correlations ($r^2 > 0.5$). Significant correlations ($P < 0.05$) are indicated with asterisks (*).

Table V: Fixed effects for GLMMs for appendicularians (AP), marine snow (MS) and fecal pellets (FP)

Model parameters	AP Coefficient	P	MS Coefficient	P	FP Coefficient	P
Temperature	0.15	0.12	0.15	0.55	−0.01	*
Salinity	−0.71	0.05	−0.31	0.8	−0.72	*
Density	0.03	0.07	0.11	0.29	−0.05	0.09
Chl*a*	0.36	**	0.95	**	0.34	*
Beam	−0.5	0.1	0.21	**	−0.52	*
AP	-	—	0.09	***	0.09	**
MS	0.53	***	—	—	0.07	0.6
FP	0.23	***	0.03	0.3	—	—

$P > 0.05 =$ ns; $P < 0.001 =$ ***; $0.001 < P < 0.05 =$ **; $P < 0.05 =$ *
Chl*a* = chlorophyll a; Beam = attenuation coefficient

and salinity. The different model runs for AP, MS and FP were significant in all cases when casts were considered as a random effect ($P < 0.05$). Although we found that Chl*a* provided the best explanation for variation of AP and MS concentrations and vertical distributions in the SJG, we cannot confirm the contribution of other factors from these models (Table V) because some of the selected variables were significantly correlated (such as density with temperature, not shown).

DISCUSSION

This study revealed and quantified the fine-scale vertical distribution of AP, MS and FP at a fixed station over 36 h in the SJG during austral summer. Furthermore, general patterns for detritus, NP and MP were also described. This was accomplished by combining the Auto-VPR and the FlowCAM®, generating a novel data set for the first time on the ACS.

Water column characteristics and their relationship with biological variables

Vertical profiles of the water column allowed us to identify a pycnocline at ∼ 40 m depth, mainly defined by temperature. The increasing water density with depth might hinder and delay gravity sedimentation of particles,

such as MS and FP. However, no clear vertical distribution pattern of them in relation to the pycnocline was observed, and only a moderate negative correlation between the water density and both MS and FP appeared. In contrast, water column density could enhance AP agglomeration above the pycnocline, as seen in the vertical distribution when high concentrations occurred. Other environmental parameters such as temperature were inversely related to density; thus, temperature was positively correlated to AP, MS and FP. In contrast, the highest concentrations of NP and MP were found in relation to lower temperature in the bottom, high salinity, high density and low Chl*a*. Daly and Smith (1993) proposed that environmental conditions enhance the formation of large-scale plankton patches, whereas biotic processes become more critical at smaller spatial scales. In our study, predation or vertical migrations may control the distribution and production of plankton over the vertical plane of the water column. As Folt and Burns (1999) described, less attention has been paid to biological processes that could facilitate plankton aggregation or patchiness compared with physical mechanisms. We found the SCML at around 20 m, which is an ecologically significant feature for planktonic ecosystems (Cullen, 2015), representing regions of high biological activity and associated with sexual reproduction and spawning events (Alldredge, 1982). Vertical distribution patterns of all our analyzed items differed overall, and we discuss

putative causes and processes associated with that in the sections below.

Appendicularians

We found AP distributed above 65 m depth of the water column, mainly above the pycnocline, with high variability in concentrations among casts. This was particularly evident at high concentrations and matching the SCML. Similar results have been documented previously, where food availability influenced AP distribution enhancing population growth (Greer *et al.*, 2013) and spawning (Alldredge, 1982). No clear agglomeration or pattern were revealed at low concentrations neither differences between day and night casts were found, suggesting the absence of DVM for AP in the SJG. *Oikopleura* spp. was the only AP genus found by Giménez *et al.* (2018) for the same sampling period, and the ones we detected with the Auto-VPR images seemed to belong to the same genus. Furthermore, the absence of clear vertical distribution patterns for AP during our study could be the consequence of different species behavior within the same genus as already reported for other areas (Shiga, 1985; Choe and Deibel, 2008). However, the number of casts performed was limited and should be increased in future studies to enlarge the number of samples, producing more replicates and cover a more extended time period to enhance support for the observation presented here.

Our results indicated negative and moderate correlations between AP and NP as well as MP, with both phytoplankton groups highly abundant in the bottom layer. Trophic links between phytoplankton and grazers, such as AP, are well known (Alldredge, 1981; Deibel and Lee, 1992; Bedo *et al.*, 1993; Lombard *et al.*, 2010; Briseño-Avena *et al.*, 2020). Since AP are non-selective grazers, they might have already efficiently grazed down NP and MP (Boltovskoy, 1981) from the layer above the pycnocline, especially when highly concentrated. The diet of AP is mainly composed of NP, and evidently, the pore size of the filtration system will determine the size range of particles on which they feed (Gorsky and Fenaux, 1998). However, grazing alone seems unlikely to produce the observed distribution patterns of NP and MP, as both also occurred in low concentrations when AP concentrations were low. Similar Chl*a* concentrations in SCML among casts without obvious decrease during our sampling period suggest that other phytoplankton groups were present in the surface layer, however, not sampled by our devices. Strictly, we cannot state that vertical distribution is related to grazing on a specific planktonic group, as we did not perform gut content analyses or grazing measurements.

Advective processes in this area, reported by Latorre *et al.* (2018) for the same period, might have also influenced AP concentrations and distributions among all casts. These authors found, at the same fixed station and sampling period, that the surface and bottom current speeds changed during one tidal cycle. Thus, horizontal physical processes could explain the low concentrations registered by the Auto-VPR during Casts 2, 5 and 6 according to low-tide and high-tide water masses changes. AP patches might have been smaller and/or their distribution less extensive spatially than that of phytoplankton. Hence, advective processes seemed not influence phytoplankton vertical distribution since the Chl*a* (as a proxy of phytoplankton biomass) profiles remained similar in all casts. Besides, higher concentrations for AP found in net samples during the same sampling time (Giménez *et al.*, 2018) suggest that Auto-VPR likely underestimates their concentrations due to small volume of water sampled at each depth.

Marine snow

We found two main patterns of MS distribution: homogeneously distributed in the water column or above the pycnocline concentrated around the SCML. The homogeneous distribution of MS aggregates throughout the water column might be explained by the place of the water column where it was produced, the age of aggregates, their consumption by several zooplankton taxa and their differential sinking rates (Lombard and Kiørboe, 2010). We observed krill FP attached to MS aggregates in some of our Auto-VPR images (Fig. 4b). With time, MS aggregates get colonized, e.g. by bacteria, phytoplankton and FP, and become heavier, making them sink rapidly (Alldredge and Silver, 1988). These aggregates are sources of strong remineralization of carbon and nutrients since they support microbial activity, becoming attractive spots for grazers, and making zones with MS ecologically relevant as feeding grounds (Alldredge *et al.*, 2002; Möller *et al.*, 2012). On the other hand, house renewal production by AP calculated in this study suggested that in at least three casts (Casts 1, 4 and 6), the order of magnitude for the MS concentration above the pycnocline could be explained by a recent house production in the surface layers, yet poorly colonized and probably sinking slowly.

Aggregates can form layers at strong density gradients due to reduced sinking rates (Alldredge *et al.*, 2002; McManus *et al.*, 2003). Distinct vertical distribution patterns for MS were reported worldwide. For example, Briseño-Avena *et al.* (2020) found that the MS (using the fluorescent particle maximum as proxy) in the North Pacific Ocean was below the SCML and formed a layer of 5–10 m thick, like MacIntyre *et al.* (1995) that described

11

accumulations of MS of 3–10 m thick. Alldredge et al. (2002) described a thin layer at 5 m depth of large aggregates of diatom-dominated MS in a North Pacific Fjord, persisting over a 24-h period and variating with the time of day and depth. Möller et al. (2012) described in the central Baltic Sea a dense thin layer of MS aggregates at the pycnocline (50–55 m), and peak concentrations of 28 particles m^{-3}, which are vastly less than the maximum peak of $\sim$ 700 particles m^{-3} that we revealed in Cast 3. They also found less dense patches of MS at some stations in the upper mixed layer, above the pycnocline. We did not find a marked discrete layer of MS. According to AP position, we reported in some casts in the upper water column, we consider that MS aggregates originated from their discarded houses and highly accumulate phytoplankton cells. At the same time, variable composition of MS might control the differential sinking rates (Laurenceau-Cornec et al., 2015). The formation of aggregates requires, besides high phytoplankton cell concentrations, low and shallow wind-induced mixing of the water column (Riebesell, 1992). These characteristics were present in the SJG and would have favored MS formation. Considering that the role and fate of MS in vertical flux are determined by its morphology and composition, Trudnowska et al. (2021) classified it into functional types and defined five MS morphotypes based on shape, darkness, size and structural heterogeneity. In this context, our aggregates seem to be mostly the «fluffy» (medium-sized, bright and with heterogeneous forms) and «agglomerated» (heterogeneous, large and bright) type. Nevertheless, we also detected fewer images of elongated (diverse in their brightness and embodying colonies of phytoplankton, filaments of cnidarians and FP) and flake-type MS (small, circular and bright). This comparison helps to elucidate the characteristics of MS, but should be used with caution since both study areas are environmentally different (SJG vs. Arctic ice marginal zones). Trudnowska et al. (2021) focused on phytoplankton blooms and composition at ice brake-up but did not report AP presence and their influence in MS formation. Moreover, we calculated MS concentration from particle numbers, which might mask the dynamics of MS when considering compression and scavenging of particles while sinking. Future studies should address these issues to clarify MS dynamics in the SJG.

Fecal pellets

We found FP throughout the water column in most casts, except in Cast 6. These FP were similar in shape to those reported by Gleiber et al. (2012) for the Antarctic euphausiid *Euphausia superba*. In the same sampling period as ours, the presence of krill larvae, juveniles and adults was found (Giménez et al., 2018, Nocera et al., 2021), and identified as individuals of *E. lucens*, *E. vallentini* and *Nematoscelis megalops*. Krill larvae and juveniles lean on AP houses and feed on the particles trapped in their mucus (Boltovskoy, 1981). Krill from the SJG was reported as herbivorous and omnivorous feeding on free phytoplankton and other zooplankton groups such as copepods (Giménez et al., 2018). We propose that krill might have also been grazing on particles, detritus and phytoplankton retained in AP houses and MS distributed overall throughout the water column, which is consistent with the krill FP distribution pattern we saw in the Auto-VPR images. We found high variability of krill FP concentration among the six casts, with highest abundances at daytime (Casts 1 and 4) that might have been produced at night during krill DVM at the surface, and likely be sinking and degrading in the meantime.

FP with associated particles might represent distinct food sources for zooplankton grazers, influencing different groups of consumers given their food selectivity (Briseño-Avena et al., 2020). Degradation of pellets might be caused by bacteria, coprorhexy and coprophagy (Iversen and Poulsen, 2007). When zooplankton consumes FP in the upper water column layers, they reduce the export of these materials to depth (Belcher et al., 2016). On the other hand, large krill FP can significantly contribute to total particulate carbon flux to depth and vary between seasons, with higher effects in summer than in winter (Gleiber et al., 2012). If FP are not consumed, they export organic particulate matter from the surface to greater depths, avoiding the recycling of materials in the upper meters (Small et al., 1979). Dissimilar sizes, compactness and types of FP have different densities and sinking rates, contributing differently to the export versus the retention of their components within the water column layers (Turner, 2015). Small FP of small mesozooplankton, as AP, are generally recycled in the water column by microbial decomposition and coprophagy (Turner, 2002). In our study, we did not detect FP from AP, which produce a great number of FP per day (López-Urrutia and Acuña, 1999). Further studies in this region should explore degradation mechanisms and FP sinking rates to figure out their role in the SJG carbon cycle.

Nano- and microplankton and small particles

Overall, we found that the NP was more abundant than MP. In the euphotic zone, both presented a good physiological state (also reported for PP in Latorre et al., 2018), but near the bottom their physiological state was poor, according to FlowCAM® images as well as flow cytometry data (G. Ferreyra, Ushuaia, personal

communication). Thus, in the bottom samples, our data might not correspond to NP and MP alive cells but rather to detritus, composed of dead phytoplankton cells, fragments of decomposed FP (by bacteria and coprorhexy) and undifferentiated nano- and microparticles. The images from the Auto-VPR revealed a wide layer (around 30 m) of small particles distributed below the pycnocline to the bottom in three of our six casts, in accordance with the high density of particles in the range of 4–20 μm analyzed with the FlowCAM® and the low beam percentage found near the bottom. Furthermore, strong and negative correlations with temperature and Chl*a* reinforce the idea that most of the NP and MP found in this study were in a degraded physiological state, probably dead cells, with a lack of floatability, accumulating in the bottom layer.

Our SCML data were not coincident with high concentrations of NP and MP, so it should correspond to another phytoplankton group. For our same fixed station and sampling period, Massé-Beaulne (2017) studied the autotroph community and reported a significant dominance of small phytoplankton in general (< 20 μm). Picocyanobacteria was the most abundant autotroph group in the surface and the SCML and significantly more abundant than picoeukaryotes, the second-most abundant group, and more abundant than NP and MP. Besides, Latorre *et al*. (2018) reported that phototrophic PP (< 4 μm) dominated the microbial community of the SJG, which might have also served as a food source for AP.

CONCLUSION

We used a combination of imagery methods to assess the *in situ* fine-scale temporal and vertical distribution of some plankton components in the SJG. A high occurrence of AP, MS and FP was found with concentrations that varied over time. When high concentrations of AP occurred, these were mainly observed above the pycnocline and correlated to the SCML, supported by a negative correlation between AP and water density. In contrast, MS and FP did not show consistent vertical distribution patterns in relation to the pycnocline. AP were strongly correlated to MS and FP when comparing three depths: surface, SCML and bottom. We found a strong positive correlation between AP and MS which is consistent with the fact that the latter usually originates from AP discarded houses. According to our MS Auto-VPR images, discarded houses of AP or their mucus fragments seemed to be the main contributors to the aggregates we report in this study. Our results showed high concentrations of nano- and micro particles near the bottom during the 36-h survey, corresponding to detritus from different origins (dead phytoplankton cells and different taxa FP, among others) that sink from the euphotic zone.

Despite being described for different regions of the global ocean, MS was previously poorly documented for the ACS, and our study represents the first one quantifying it in the SJG. MS aggregates might be an essential food source in bentho-pelagic coupling, not previously considered, to our knowledge, in the Patagonian region. Further efforts should be made to characterize the MS composition and the microbial community inhabiting these aggregates, and to determine their local concentrations throughout time and space. In addition, a better understanding of the ecological role that MS plays in the Patagonian pelagic food web is essential to elucidate the carbon export and final sequestration in sediments. This is extremely important in shallow continental shelves, where particle sedimentations reach the bottom faster when compared with the open ocean.

SUPPLEMENTARY DATA

Supplementary data is available at *Journal of Plankton Research* online.

DATA AVAILABILITY

Data available on request from the authors.

REFERENCES

Abraham, E. R. (1998) The generation of plankton patchiness by turbulent stirring. *Nature*, **391**, 577–580. https://doi.org/10.1038/35361.

Akselman, R. (1996) *Estudios ecológicos en el Golfo San Jorge Y Adyacencias (Atlántico Sudoccidental). Distribución, Abundancia Y variación Estacional del Fitoplancton en relación a Factores físico-químcos Y la dinámica hidrológica.* PhD Thesis, Universidad de Buenos Aires, Buenos Aires, Argentina, p. 244.

Alldredge, A. L. (1976) Field behavior and adaptive strategies of appendicularians (Chordata: Tunicata). *Mar. Biol.*, **38**, 29–39. https://doi.org/10.1007/BF00391483.

Alldredge, A. L. (1981) The impact of appendicularian grazing on natural food concentrations in situ. *Limnol. Oceanogr.*, **26**, 247–257. https://doi.org/10.4319/lo.1981.26.2.0247.

Alldredge, A. L. (1982) Aggregation of spawning appendicularians in surface windrows. *B. Mar. Sci.*, **32**, 250–254.

Alldredge, A. L., Cowles, T. J., MacIntyre, S., Rines, J. E. B., Donaghay, P. L., Greenlaw, C. F., Holliday, D. V., Dekshenieks, M. M. *et al.* (2002) Occurrence and mechanisms of formation of a dramatic thin layer of marine snow in a shallow Pacific fjord. *Mar. Ecol. Prog. Ser.*, **233**, 1–12. https://doi.org/10.3354/meps233001.

Alldredge, A. L. and Jackson, G. A. (1995) Preface: aggregation in marine system. *Deep Sea Res. II*, **42**, 1–7. https://doi.org/10.1016/0967-0645(95)90003-9.

Alldredge, A. L., Passow, U. and Logan, B. E. (1993) The abundance and significance of a class of large, transparent organic particles in the ocean. *Deep Sea Res. I*, **40**, 1131–1140. https://doi.org/10.1016/0967-0637(93)90129-Q.

Alldredge, A. L. and Silver, M. W. (1988) Characteristics, dynamics and significance of marine snow. *Prog. Oceanogr.*, **20**, 41–82. https://doi.org/10.1016/0079-6611(88)90053-5.

Atkinson, A., Schmidt, K., Fielding, S., Kawaguchi, S. and Geissler, P. A. (2012) Variable food absorption by Antarctic krill: relationships between diet, egestion rate and the composition and sinking rates of their fecal pellets. *Deep Sea Res. II*, **59-60**, 147–158. https://doi.org/10.1016/j.dsr2.2011.06.008.

Azam, F., Fenchel, T., Field, J. G., Gray, J. S., Meyer-Reil, L. A. and Thingstad, F. (1983) The ecological role of water-column microbes in the sea. *Mar. Ecol. Prog. Ser.*, **10**, 257–263. https://doi.org/10.3354/meps010257.

Bedo, A. W., Acuna, J. L., Robins, D. and Harris, R. P. (1993) Grazing in the micron and the sub-micron particle size range: the case of *Oikopleura dioica* (Appendicularia). *B. Mar. Sci.*, **53**, 2–14.

Belcher, A., Iversen, M., Manno, C., Henson, S. A., Tarling, G. A. and Sanders, R. (2016) The role of particle associated microbes in remineralization of faecal pellets in the upper mesopelagic of the Scotia Sea, Antarctica. *Limnol. Oceanogr.*, **61**, 1049–1064. https://doi.org/10.1002/lno.10269.

Benfield, M. C., Davis, C. S., Wiebe, P. H., Gallager, S. M., Gregory Loughj, R. and Copley, N. J. (1996) Video plankton recorder estimates of copepod, pteropod and larvacean distributions from a stratified region of Georges Bank with comparative measurements from a MOCNESS sampler. *Deep Sea Res. II*, **43**, 1925–1945. https://doi.org/10.1016/S0967-0645(96)00044-6.

Bianchi, A. A., Bianucci, L., Piola, A. R., Pino, D. R., Schloss, I., Poisson, A. and Balestrini, C. F. (2005) Vertical stratification and air-sea CO2 fluxes in the Patagonian shelf. *J. Geophys. Res.*, **110**, C07003.

Boltovskoy, D. (1981) *Atlas del Zooplancton del Atlántico Sudoccidental Y métodos de Trabajo Con el Zooplancton Marino*, Instituto Nacional de Investigación y Desarrollo Pesquero, Buenos Aires, Argentina: Mar del Plata, p. 936.

Briseño-Avena, C., Prairie, J. C., Franks, P. J. and Jaffe, J. S. (2020) Comparing vertical distributions of chl-a fluorescence, marine snow, and taxon-specific zooplankton in relation to density using high-resolution optical measurements. *Front. Mar. Sci.*, **7**, 1–15. https://doi.org/10.3389/fmars.2020.00602.

Capitanio, F., Pájaro, M. and Esnal, G. B. (1997) Appendicularians (Chordata, Tunicata) in the diet of anchovy *Engraulis anchoita* in the argentine sea. *Sci. Mar.*, **61**, 9–15.

Capitanio, F., Pájaro, M. and Esnal, G. B. (2005) Appendicularians: an important food supply for the argentine anchovy *Engraulis anchoita* in coastal waters. *J. Appl. Ichthyol.*, **21**, 414–419. https://doi.org/10.1111/j.1439-0426.2005.00657.x.

Capitanio, F. L. and Esnal, G. B. (1998) Vertical distribution of maturity stages of *Oikopleura dioica* (Tunicata, Appendicularia) in the frontal system off Valdés peninsula, Argentina. *Bull. Mar. Sci.*, **63**, 531–539.

Cepeda, G. D., Temperoni, B., Sabatini, M. E., Viñas, M. D., Derisio, C. M., Santos, B. A., Antacli, J. C. and Padovani, L. N. (2018) Zooplankton communities of the Argentine continental shelf (SW Atlantic, ca. 34°-55°S), an overview. In: Hoffmeyer, M., Sabatini, M., Brandini, F., Calliari, D., Santinelli, N. (eds.), *Plankton Ecology of the Southwestern Atlantic*. Springer, Cham, pp. 171–199, https://doi.org/10.1007/978-3-319-77869-3_9.

Choe, N. and Deibel, D. (2008) Temporal and vertical distributions of three appendicularian species (Tunicata) in Conception Bay, Newfoundland. *J. Plankton Res.*, **30**, 969–979. https://doi.org/10.1093/plankt/fbn064.

Cullen, J. J. (2015) Subsurface chlorophyll maximum layers: enduring enigma or mystery solved? *Annu. Rev. Mar. Sci.*, **7**, 207–239. https://doi.org/10.1146/annurev-marine-010213-135111.

Daly, K. L. and Smith, W. O. (1993) Physical-biological interactions influencing marine plankton production. *Annu. Rev. Ecol. Syst.*, **24**, 555–585. https://doi.org/10.1146/annurev.es.24.110193.003011.

Davis, C. S., Gallager, S. M. and Solow, A. R. (1992) Microaggregations of oceanic plankton observed by towed video microscopy. *Science*, **257**, 230–232. https://doi.org/10.1126/science.257.5067.230.

Deibel, D. (1986) Feeding mechanism and house of the appendicularian *Oikopleura vanhoeffeni*. *Mar. Biol.*, **93**, 429–436. https://doi.org/10.1007/BF00401110.

Deibel, D. and Lee, S. H. (1992) Oikopleura vanhoeffeni. *Mar. Ecol. Prog. Ser.*, **81**, 25–30. https://doi.org/10.3354/meps081025.

Dunbar, R. B. and Berger, W. H. (1981) Fecal pellet flux to modern bottom sediment of Santa Barbara Basin (California) based on sediment trapping. *Geol. Soc. Am. Bull.*, **92**, 212–218. https://doi.org/10.1130/0016-7606(1981)92<212:FPFTMB>2.0.CO;2.

Esnal, G. B. (1999) Appendicularia. In Boltovskoy, D. (ed.), *Atlas del Zooplancton del Atlántico Sudoccidental Y métodos de Trabajo Con el Zooplancton Marino*, Publicación especial INIDEP, Mar del Plata, pp. 809–827.

Fenchel, T. (1988) Marine plankton food chains. *Annu. Rev. Ecol. Syst.*, **19**, 19–38. https://doi.org/10.1146/annurev.es.19.110188.000315.

Flood, P. R., Deibel, D. and Morris, C. (1992) Filtration of colloidal melanin from seawater by planktonic tunicates. *Nature*, **355**, 630–632. https://doi.org/10.1038/355630a0.

Folt, C. and Burns, C. (1999) Biological drivers of zooplankton patchiness. *Trends Ecol. Evol.*, **14**, 300–305. https://doi.org/10.1016/S0169-5347(99)01616-X.

Gallager, S. M., Yamazaki, H. and Davis, C. S. (2004) Contribution of fine-scale vertical structure and swimming behavior to formation of plankton layers on Georges Bank. *Mar. Ecol. Prog. Ser.*, **267**, 27–43. https://doi.org/10.3354/meps267027.

Giménez, E. M., Winkler, G., Hoffmeyer, M. and Ferreyra, G. (2018) Composition, spatial distribution, and trophic structure of the zooplankton community in San Jorge Gulf, Southwestern Atlantic Ocean. *Oceanography*, **31**, 154–163. https://doi.org/10.5670/oceanog.2018.418.

Gleiber, M. R., Steinberg, D. K. and Ducklow, H. W. (2012) Time series of vertical flux of zooplankton fecal pellets on the continental shelf of the western Antarctic peninsula. *Mar. Ecol. Prog. Ser.*, **471**, 23–36. https://doi.org/10.3354/meps10021.

Glembocki, N. G., Williams, N. G., Góngora, M. E., Gagliardini, D. A. and Orensanz, J. M. (2015) Synoptic oceanography of San Jorge Gulf (Argentina): a template for Patagonian red shrimp (*Pleoticus muelleri*) spatial dynamics. *J. Sea Res.*, **95**, 22–35. https://doi.org/10.1016/j.seares.2014.10.011.

Góngora, M. E., González-Zevallos, D., Pettovello, A. and Mendia, L. (2012) Caracterización de las principales pesquerías del Golfo san Jorge Patagonia, Argentina. *Lat. Am. J. Aquat. Res.*, **40**, 1–11. https://doi.org/10.3856/vol40-issue1-fulltext-1.

Gorsky, G. and Fenaux, R. (1998) The role of appendicularia in marine food webs. In Bone, Q. (ed.), *The Biology of Pelagic Tunicates*, Oxford University Press, Oxford, pp. 161–170.

Greer, A. T., Cowen, R. K., Guigand, C. M., McManus, M. A., Sevadjian, J. C. and Timmerman, A. H. (2013) Relationships between phytoplankton thin layers and the fine-scale vertical distributions of two trophic levels of zooplankton. *J. Plankton Res.*, **35**, 939–956. https://doi.org/10.1093/plankt/fbt056.

Irigoien, X., Conway, D. V. and Harris, R. P. (2004) Flexible diel vertical migration behaviour of zooplankton in the Irish Sea. *Mar. Ecol. Prog. Ser.*, **267**, 85–97. https://doi.org/10.3354/meps267085.

Iversen, M. H. and Poulsen, L. K. (2007) Coprorhexy, coprophagy, and coprochaly in the copepods *Calanus helgolandicus*, *Pseudocalanus elongatus*, and *Oithona similis*. *Mar. Ecol. Prog. Ser.*, **350**, 79–89. https://doi.org/10.3354/meps07095.

Jakobsen, H. H. and Carstensen, J. (2011) FlowCAM: sizing cells and understanding the impact of size distributions on biovolume of planktonic community structure. *Aquat. Microb. Ecol.*, **65**, 75–87. https://doi.org/10.3354/ame01539.

Kiørboe, T. (2000) Colonization of marine snow aggregates by invertebrate zooplankton: abundance, scaling, and possible role. *Limnol. Oceanogr.*, **45**, 479–484. https://doi.org/10.4319/lo.2000.45.2.0479.

Krock, B., Borel, C. M., Barrera, F., Tillmann, U., Fabro, E., Almandoz, G. O., Ferrario, M., Garzón Cardona, J. E. *et al.* (2015) Analysis of the hydrographic conditions and cyst beds in the San Jorge Gulf, Argentina, that favor dinoflagellate population development including toxigenic species and their toxins. *J. Mar. Syst.*, **148**, 86–100. https://doi.org/10.1016/j.jmarsys.2015.01.006.

Lampitt, R. S., Wishner, K. F., Turley, C. M. and Angel, M. V. (1993) Marine snow studies in the Northeast Atlantic Ocean: distribution, composition and role as a food source for migrating plankton. *Mar. Biol.*, **116**, 689–702. https://doi.org/10.1007/BF00355486.

Latorre, M. P., Schloss, I. R., Almandoz, G. O., Lemarchand, K., Flores-Melo, X., Massé-Beaulne, V. and Ferreyra, G. (2018) Mixing processes at the pycnocline and vertical nitrate supply: consequences for the microbial food web in San Jorge Gulf, Argentina. *Oceanography*, **31**, 50–59. https://doi.org/10.5670/oceanog.2018.410.

Laurenceau-Cornec, E. C., Trull, T. W., Davies, D. M., Bray, S. G., Doran, J., Planchon, F., Carlotti, F., Jouandet, M. P. *et al.* (2015) The relative importance of phytoplankton aggregates and zooplankton fecal pellets to carbon export: insights from free-drifting sediment trap deployments in naturally iron-fertilised waters near the Kerguelen plateau. *Biogeosciences*, **12**, 1007–1027. https://doi.org/10.5194/bg-12-1007-2015.

Lombard, F., Eloire, D., Gobet, A., Stemmann, L., Dolan, J. R., Sciandra, A. and Gorsky, G. (2010) Experimental and modelling evidence of appendicularian-ciliate interactions. *Limnol. Oceanogr.*, **55**, 77–90. https://doi.org/10.4319/lo.2010.55.1.0077.

Lombard, F. and Kiørboe, T. (2010) Marine snow originating from appendicularians houses: age-dependent settling characteristics. *Deep Sea Res. I*, **57**, 1304–1313. https://doi.org/10.1016/j.dsr.2010.06.008.

Longhurst, A. R. and Harrison, G. W. (1989) The biological pump: profiles of plankton production and consumption in the upper ocean. *Prog. Oceanogr.*, **22**, 47–123. https://doi.org/10.1016/0079-6611(89)90010-4.

López-Urrutia, Á. and Acuña, J. L. (1999) Gut throughput dynamics in the appendicularians *Oikopleura dioica*. *Mar. Ecol. Prog. Ser.*, **191**, 195–205. https://doi.org/10.3354/meps191195.

Lundgreen, R. B., Jaspers, C., Traving, S. J., Ayala, D. J., Lombard, F., Grossart, H. P., Nielsen, T. G., Munk, P. *et al.* (2019) Eukaryotic and cyanobacterial communities associated with marine snow particles in the oligotrophic Sargasso Sea. *Sci. Rep.*, **9**, 1–12.

MacIntyre, S., Alldredge, A. L. and Gotschalk, C. C. (1995) Accumulation of marines now at density discontinuities in the water column. *Limnol. Oceanogr.*, **40**, 4049–4468.

Manual Digital Auto VPRII (2010) *Operation and Maintenance of the Digital AutoVPRII*, Falmouth, Massachusetts, U.S: Seascan, Inc., p. 25.

Massé-Beaulne, V. (2017) *Métabolisme de la comumunauté Microbienne et Flux de Carbone à Court Terme Dans le Golfe San Jorge, Patagonie (Argentine)*MSc. Thesis,, Université du Québec à Rimouski, Québec, Canada, p. 121.

McManus, M. A., Alldredge, A. L., Barnard, A. H., Boss, E., Case, J. F., Cowles, T. J., Donaghay, P. L., Eisner, D. J. *et al.* (2003) Characteristics, distribution and persistence of thin layers over a 48 hour period. *Mar. Ecol. Prog. Ser.*, **261**, 1–19. https://doi.org/10.3354/meps261001.

McManus, M. A., Cheriton, O. M., Drake, P. J., Holliday, D. V., Storlazzi, C. D., Donaghay, P. L. and Greenlaw, C. F. (2005) Effects of physical processes on structure and transport of thin zooplankton layers in the coastal ocean. *Mar. Ecol. Prog. Ser.*, **301**, 199–215. https://doi.org/10.3354/meps301199.

Möller, K. O., John, M. S., Temming, A., Floeter, J., Sell, A. F., Herrmann, J. P. and Möllmann, C. (2012) Marine snow, zooplankton and thin layers: indications of a trophic link from small-scale sampling with the video plankton recorder. *Mar. Ecol. Prog. Ser.*, **468**, 57–69. https://doi.org/10.3354/meps09984.

Nishibe, Y., Takahashi, K., Ichikawa, T., Hidaka, K., Kurogi, H., Segawa, K. and Saito, H. (2015) Degradation of discarded appendicularians houses by oncaeid copepods. *Limnol. Oceanogr.*, **60**, 967–976. https://doi.org/10.1002/lno.10061.

Nocera, A. C., Giménez, E. M., Diez, M. J., Retana, M. V. and Winkler, G. (2021) Krill diel vertical migration in southern Patagonia. *J. Plankton Res.*, **43**, 610–623. https://doi.org/10.1093/plankt/fbab047.

Parsons, T. R., Maita, Y. and Lalli, C. M. (1984) *A Manual of Chemical and Biological Methods for Seawater Analysis*, Pergamon Press, Oxford, New York, p. 173.

Pérez Seijas, G. M., Ramírez, F. C. and Viñas, M. D. (1987) Variaciones de la abundancia numérica y biomasa del zooplancton de red en el golfo san Jorge (Año 1985). *Rev. Invest. Des. Pesq.*, **7**, 5–20.

R Development Core Team (2019) *R: A Language and Environment for Statistical Computing*, R Foundation for Statistical Computing, Vienna, Austria.

Riebesell, U. (1992) The formation of large marine snow and its sustained residence in surface waters. *Limnol. Oceanogr.*, **37**, 63–76. https://doi.org/10.4319/lo.1992.37.1.0063.

Sato, R., Ishibashi, Y., Tanaka, Y., Ishimaru, T. and Dagg, M. J. (2008) Productivity and grazing impact of *Oikopleura dioica* (Tunicata, Appendicularia) in Tokyo Bay. *J. Plankton Res.*, **30**, 299–309.

Sato, R., Tanaka, Y. and Ishimaru, T. (2001) House production by *Oikopleura dioica* (Tunicata, Appendicularia) under laboratory conditions. *J. Plankton Res.*, **23**, 415–423. https://doi.org/10.1093/plankt/23.4.415.

Segura, V. and Silva, R. (2017) Producción primaria y su relación con los grupos fitoplanctónicos en el periodo de primavera en el Golfo san Jorge y área adyacente, Argentina. *INIDEP Tech. Rep.*, **30**, 1–33.

Shiga, N. (1985) Seasonal and vertical distributions of appendicularia in Volcano Bay, Hokkaido, Japan. *Bull. Mar. Sci.*, **37**, 425–439.

Small, L. F., Fowler, S. W. and Ünlü, M. Y. (1979) Sinking rates of natural copepod fecal pellets. *Mar. Biol.*, **51**, 233–241. https://doi.org/10.1007/BF00386803.

Spinelli, M., Derisio, C., Martos, P., Pájaro, M., Esnal, G., Mianzán, H. and Capitanio, F. (2015) Diel vertical distribution of the larvacean *Oikopleura dioica* in a north Patagonian tidal frontal system (42°–45° S) of the SW Atlantic Ocean. *Mar. Biol. Res.*, **11**, 633–643. https://doi.org/10.1080/17451000.2014.978338.

Tomita, M., Shiga, N. and Ikeda, T. (2003) Seasonal occurrence and vertical distribution of appendicularians in Toyama Bay, southern Japan Sea. *J. Plankton Res.*, **25**, 579–589. https://doi.org/10.1093/plankt/25.6.579.

Trudnowska, E., Lacour, L., Ardyna, M., RTogge, A., Irisson, J. O., Waite, A. M., Babin, M. and Stemmann, L. (2021) Marine snow morphology illuminates the evolution of phytoplankton blooms and determines their subsequent vertical export. *Nat. Commun.*, **12**, 2816. https://doi.org/10.1038/s41467-021-22994-4.

Turner, J. T. (2002) Zooplankton fecal pellets, marine snow and sinking phytoplankton blooms. *Aquat. Microb. Ecol.*, **27**, 57–102. https://doi.org/10.3354/ame027057.

Turner, J. T. (2004) The importance of small planktonic copepods and their roles in pelagic marine food webs. *Zool. Stud.*, **43**, 255–266.

Turner, J. T. (2015) Zooplankton fecal pellets, marine snow, phytodetritus and the ocean's biological pump. *Prog. Oceanogr.*, **130**, 205–248. https://doi.org/10.1016/j.pocean.2014.08.005.

Verdugo, P. (2012) Marine microgels. *Annu. Rev. Mar. Sci.*, **4**, 375–400. https://doi.org/10.1146/annurev-marine-120709-142759.

Wells, M. L. (1998) A neglected dimension. *Nature*, **391**, 530–531.